Electromagnetic properties of hollandite $K_2V_8O_{16}$ under pressure

Touru Yamauchi,* Hiroaki Ueda, Masahiko Isobe, and Yutaka Ueda
Material Design and Characterization Laboratory, Institute for Solid State Physics, University of Tokyo, 5-1-5 Kashiwanoha, Kashiwa, Chiba 277-8581, Japan
(Received 4 May 2011; published 9 September 2011)

The magnetic susceptibility and resistivity of V^{4+}/V^{3+} mixed-valence vanadium oxide (hollandite $K_2V_8O_{16}$) were measured under pressure. The resistivity measurements show that the charge-order transition temperature (T_{CO}) is suppressed with increasing pressure up to 1 GPa, as observed in many kinds of charge-ordering compounds. At 1 GPa, the pressure dependence of T_{CO} suddenly changes its tendency; further compression of the system above 1 GPa leads T_{CO} to higher temperatures. This clearly shows an appearance of a new ground state at around 1 GPa. This situation is also revealed by dc-susceptibility measurements: The nonmagnetic ambient ground state suddenly turns into a magnetic state at around 1 GPa. These high-pressure experimental results could be explained as a switching between two kinds of orbital-charge-spin ordered structures.

DOI: 10.1103/PhysRevB.84.115104 PACS number(s): 71.30.+h, 74.62.Fj

I. INTRODUCTION

The metal-to-insulator transition (MIT) is a fascinating phenomenon in solids. Many MITs have been observed as a function of temperature. Particularly, MITs in mixed-valence compounds are considered as charge-ordering (CO) transitions, as typically seen in mixed-valence vanadium oxides. Hollandite, $K_2V_8O_{16}$, V^{4+}/V^{3+} mixed-valence vanadium oxide is a new addition to CO compounds in which MIT has been recently observed.[1] At ambient pressure, this MIT is accompanied by a steep decrease in magnetic susceptibility and the appearance of a $\sqrt{2}a \times \sqrt{2}a \times 2c$ super lattice. This MIT is complex because the resistivity-temperature (ρ-T) curve shows two-step-like behavior at the transition indicating complex phase relations. In this work, not only the overall behavior of the CO phase under pressure but also phase relations under high pressure will be made clear.

At ambient pressure and room temperature, the tetragonal crystal structure of hollandite $K_2V_8O_{16}$ (inset of Fig. 1) has a V_8O_{16} framework formed by double strings of edge-shared VO_6 octahedra. The K^+ ions settle at the center of the square, with straight tunnels along the c axis. The structure symmetry is given by $I4/m$, and the V atoms share a crystallographically identical $8h$ site.[2] Therefore, the good metallic behavior is well explained by the mixed-valence state of vanadium atoms: $V^{3.75+}$, $V^{3+}(3d^2)/V^{4+}(3d^1) = 1/3$. This charge degree of freedom possibly plays a key role in the observed complex MIT.

Here, we note some detailed electromagnetic properties of this compound at ambient pressure.[3] As briefly mentioned above, the ρ-T curve at around the MIT shows peculiar two-step-like behavior. Hereafter, we will represent the transition temperatures of the first step (higher transition temperature) as T_{CO}^h and the second step (the lower one) as T_{CO}^l. At ambient pressure, these two transitions were observed at $T_{CO}^h = 180 \pm 10$ and $T_{CO}^l = 150 \pm 5$ K (sample dependence is observed). Above T_{CO}^h, namely above the MIT temperature, the system shows a good metallicity of several hundred $\mu\Omega$ cm only along the c axis and slightly insulating behavior along the a axis. Anisotropy of the resistivity, ρ_a/ρ_c (including dimensional error), is approximately at unity at room temperature, $3 \sim 4$ at just above T_{CO}^h, and unity again below T_{CO}^l. Some other experimental observations, such as magnetic susceptibility and x-ray diffraction, also show the existence of a "mid-step" phase between T_{CO}^h and T_{CO}^l. However, in contrast to the CO ground state below T_{CO}^l, the crystallographic properties of the mid-step phase remain unidentified due to the overlap of x-ray scattering spots (probably resulting from the twin structure of the crystal). The ambient magnetic susceptibility-temperature (χ-T) curve exhibits Curie-Weiss behavior in the metallic phase, a moderate drop between T_{CO}^h and T_{CO}^l, and a steep drop at T_{CO}^l to low χ value, which seems to show a spin-singlet feature of the CO ground state. Below 50 K, an extrinsic small Curie tail can be seen on the χ-T curve. Careful measurements of warming-up and cooling-down hysteresis of χ-T curves near the transition reveal the mid-step phase (for this observation, a sufficiently large and uniform single crystal is required).

In this study, we have performed high-pressure experiments using single crystals. These sample crystals have some heterogeneity which appears as differences of T_{CO}^h and/or T_{CO}^l (20 K at the most), depending on the sample pieces. This is probably due to nonstoichiometry of the K ion. It should be noted that the synthesis and crystal growth have to be performed under a pressure of about 4 GPa. Despite this inevitable sample dependence, we will reveal some common and essential electromagnetic properties of this compound under pressure and discuss the peculiar pressure-temperature (P-T) phase diagram.

II. EXPERIMENTAL

Powder samples of $K_2V_8O_{16}$ were prepared by a solid-state reaction of KVO_3, V_2O_3, and V_2O_5 under 4 GPa at 1200 °C for one hour.[1] Starting reagents were ground thoroughly and the mixture was wrapped in platinum foil and put into a pressure cell. KVO_3 was obtained by a reaction of K_2CO_3 and V_2O_5. V_2O_3 was prepared by reducing V_2O_5 under H_2 gas flow at 900 °C. A cubic-type apparatus was used for the high-pressure synthesis. Sample identification was performed using powder x-ray diffraction. Very small single crystals were found in the sintered sample. The largest and typical sizes of the crystals were $0.3 \times 0.3 \times 0.8$ mm^3 and $0.1 \times 0.1 \times 0.3$ mm^3, respectively.

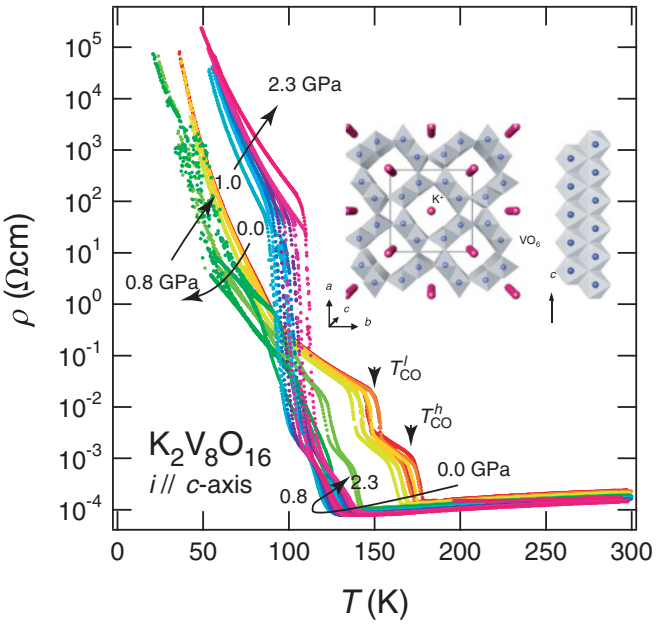

FIG. 1. (Color online) A set of several resistivity-temperature (ρ-T) curves up to 2.3 GPa. Near ambient pressure, ρ-T curves show the characteristic two-step-like behavior (red and yellow curves) near the MIT. At 0.8 $\sim$ 1.0 GPa, drastic change was observed (green and sky blue). The crystal structure of hollandite, $K_2V_8O_{16}$, projected along the c axis, is illustrated in the inset. It consists of a V_8O_{16} framework formed by "edge-shared" double chains and K ions (small red balls) in the tunnel sites.

The resistivity of a single crystal along the c axis (tunnel direction) was measured by an ordinary 4-probe method in two types of pressure apparatus with the following constant dc excitation currents: 0.1 μA, 10 μA, and 1 mA. One is a piston-cylinder type (up to 2.3 GPa), and the other is a cubic-anvil type (up to 8.2 GPa). We employed Daphne oil 7373 (Idemitsu Co., Ltd.) as a pressure medium in the piston-cylinder cell and adopted a methanol-ethanol mixture (4:1) drop method in cubic-anvil-type cell to ensure good hydrostaticity.[4] Incidentally, favorable electric contact with sample crystals of $K_2V_8O_{16}$ requires rapid wiring to the fresh crystal surface immediately after extraction from a high-pressure synthesis cell.

The magnetic susceptibility χ of the largest single crystal (about 2 mg) under various pressures was measured in an external field of 1T using a commercial magnetometer (MPMS-5s, Quantum Design Co., Ltd.) equipped with a pressure cell made of a CuBe cylinder and ZrO_2 pistons. Daphne oil 7373 (Idemitsu Co., Ltd.) was used as a pressure medium. In these measurements, the contribution from the pressure cell filled with Daphne oil without sample was subtracted from the raw output signals of the MPMS *in situ*.[5] The magnetization was measured along the c axis.

III. RESULTS

A. Resistivity measurements

Resistivity measurement is the most popular way to explore the electronic state of material especially under high-pressure conditions. $K_2V_8O_{16}$ is one of the good target compounds for measuring resistivity as it allows us to observe its significant MIT. The observed ρ-T curves at several constant pressures from 0.0 to 2.3 GPa are illustrated in Fig. 1. The rainbow colors identify the pressures [0.0 (red) $\rightarrow$ 2.3 GPa (purple)]. Although detailed notations for pressure identification are omitted for simplicity in this figure (these will be seen in a later part of this paper), one can see the characteristic pressure evolution of ρ-T curves between 0.8 $\sim$ 1.0 GPa.

From 0.0 to 0.8 GPa, both steps in a peculiar two-step MIT on the ρ-T curves are shifted to a lower temperature with increasing pressure. The mid-step width, namely $T^h_{CO} - T^l_{CO}$, becomes narrower, and the two steps seem to merge at around 0.8 GPa as shown later. The most significant change of ρ-T curves occurs between 0.8 $\sim$ 1.0 GPa; the magnitudes of the difference of ρ just below and above the MIT (below and above the two steps) are 10^2 below 0.8 GPa and 10^6 above 1.0 GPa, respectively. Moreover, the pressure dependence of the T_{CO} changes its tendency at the critical pressure (P_c = 0.8 $\sim$ 1.0 GPa); T_{CO} is lowered below P_c and slightly shifts to higher above P_c with increasing pressure. These aspects reveal a switching between at least two kinds of ground states by applying pressure.

The Arrhenius plot is useful in displaying the electronic properties of the insulating ground states such as CO phases. A set of ρ-T curves in Fig. 1 is redrawn as an Arrhenius plot in the inset of Fig. 2. A color set of ρ-T curves for pressure identification is the same as that in Fig. 1. In this plot, the drastic change of the ρ-T curve at P_c is also clearly seen as a jump of ρ at low temperature by several orders of magnitude. The low-temperature section of the ρ-T curves can be explained by a simple band-gap picture (shown by broken lines in this figure) excepting the several ρ-T curves observed near P_c. These exceptional ρ-T curves show a variable-range-hopping (VRH) nature rather than simple gap behavior. Moreover, the electric conduction of $K_2V_8O_{16}$ at low temperature near the P_c is a *non*-ohmic one. This leads us to suppose some analogy with the organic thyristor discussed as a competition or coexistence

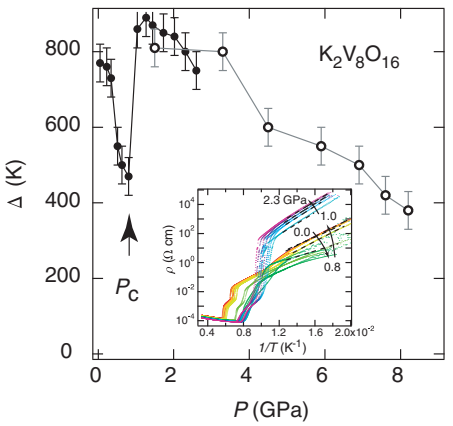

FIG. 2. (Color online) The pressure dependence of gap energy (Δ) of the CO state obtained from an Arrhenius plot of the set of ρ-T curves. The closed and open circles show the Δ obtained from high-pressure experiments using a piston-cylinder and a cubic-anvil cell (the ρ-T not shown here), respectively. The inset shows an Arrhenius plot of the set of ρ-T curves. The rainbow color represents the pressure sequence in the same manner as Fig. 1.

of two types of CO phases in the system.[6] It appears that both voltage-current characteristics and generating alternating current by applying a static direct-current voltage, which are essential aspects in a thyristor, present interesting future work in this vanadium hollandite system.

The main panel of Fig. 2 shows the pressure dependence of the estimated energy gap (Δ) from an Arrhenius plot of ρ-T curves. The closed and open symbols are derived from piston-cylinder and cubic-anvil type (ρ-T, not shown in this figure) high-pressure experiments, respectively. At ambient pressure, Δ is estimated at about 800 K and steeply decreases with increasing pressure. Strictly speaking, ρ-T near the P_c has a slight convex shape in the Arrhenius plot at low temperatures. The estimated Δ is about 440 K, even though the VRH picture is more suitable for electric conduction in this pressure region. At the P_c, Δ suddenly jumps up to about 850 K, and the simple gap behavior reappears. As pressure is increased up to 8.2 GPa, Δ decreases monotonically down to about 400 K.

In order to see the detailed pressure evolution of the peculiar two-step MIT up to 8.2 GPa, the ρ-T curves in the range of 50 $\sim$ 250 K are shown in Fig. 3 with appropriate offset for easy viewing. In this figure, the ρ-T curves obtained in two

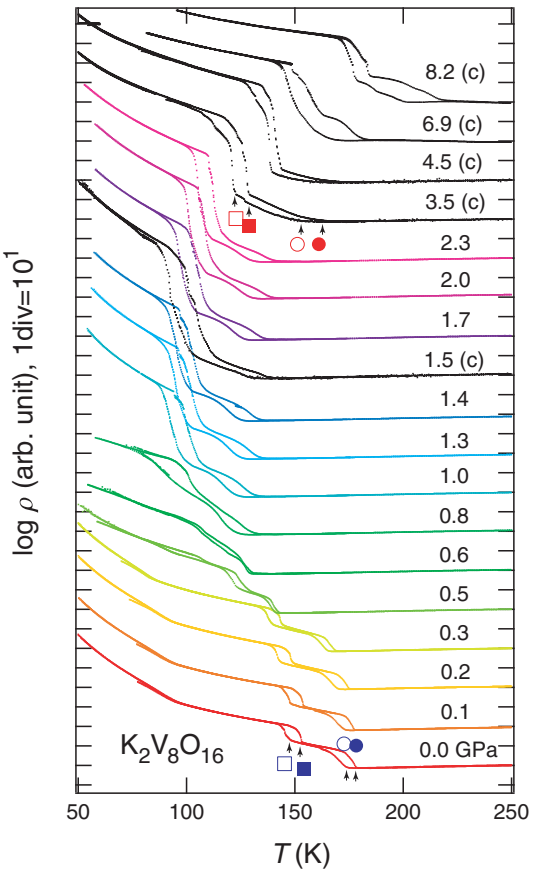

FIG. 3. (Color online) The pressure evolution of the characteristic two-step-like transition in ρ-T curves up to 8.2 GPa. The rainbow color and black curves [with the notation of "(c)"] are obtained from piston-cylinder and cubic-anvil experiments, respectively. The open/closed and circle/square symbols represent the transition temperatures (see the text) which are plotted in the P-T phase diagram (Fig. 5).

types of high-pressure experiments using piston-cylinder (with rainbow colors) and cubic-anvil type (black) high-pressure cells are represented. One can see the notations for pressure identification, which have been omitted in previous figures, on every ρ-T curve. There are several other kinds of symbols in this figure. The circle and square represent phase transition temperatures, T_{CO}^h and T_{CO}^l, respectively. The open/closed symbols show the transition temperatures observed in the cooling/warming processes, respectively. These symbols will appear again in the P-T phase diagram discussed later in this paper.

It is natural to observe temperature hysteresis on ρ-T curves in the case of first-order transitions. Therefore, the transitions at T_{CO}^h and T_{CO}^l (represented by circle and square symbols, respectively) are first-order transitions. The typical hysteresis width is about 5 K at ambient pressure for both transitions. With increasing pressure up to 0.5 GPa, the MIT shifts to a lower temperature, and the two steps are clearly seen. At 0.6 GPa, the two steps become hardly distinguishable, and the hysteresis almost merges. At 0.8 GPa, large hysteresis with a different two-step shape appears again. At 1.0 GP, a clearer two steps are observed. These two-step transitions below and above the P_c are probably transitions from a high-temperature common metallic phase to different low-temperature CO phases, respectively. Above 1.0 GPa, the newly observed two-step transitions (the transition temperatures will again be denoted as T_{CO}^h and T_{CO}^l) shift to higher temperature with increasing pressure.

The presence of another kind of CO ground state above the P_c can be expected because the magnitude of difference of ρ just above and below the two-step MIT suddenly increases from 10^2 to 10^6 at the P_c (note that one tick in the vertical axis of this figure denotes 10^1). Another reason is that the pressure dependencies of both T_{CO}^h and T_{CO}^l change their tendencies; they decrease below the P_c and increase above the P_c with pressure. This should be additional important evidence for the appearance of a new ground state above the P_c. From these pressure dependencies, we can also expect at least two types of mid-step phases below and above the P_c.

B. Susceptibility measurements

Magnetic susceptibility measurement is another useful tool to explore high-pressure states of materials, even though the observation of small magnetic signals, as with $K_2V_8O_{16}$, is restricted to lower-than-capable pressure in a piston-cylinder pressure cell. Thus, we have performed susceptibility measurements using a single crystal up to 1.4 GPa, which is sufficient to observe the magnetic properties near and above the P_c.

The observed magnetic susceptibility versus temperature (χ-T) curves under several constant pressures up to 1.4 GPa are shown in Fig. 4. The rainbow colors identify the pressure where the χ-T curve is measured. With the exception of some notations which are important to understand the tendency of pressure evolution of the χ-T curves, detailed notations are omitted for simplicity in this figure.

By lowering temperature, the ambient χ-T curve shows a kink at 170 K (a closed circle) and a sudden drop at 150 K (a closed square), corresponding to the first and second steps on the ρ-T curve, respectively. Careful temperature hysteresis

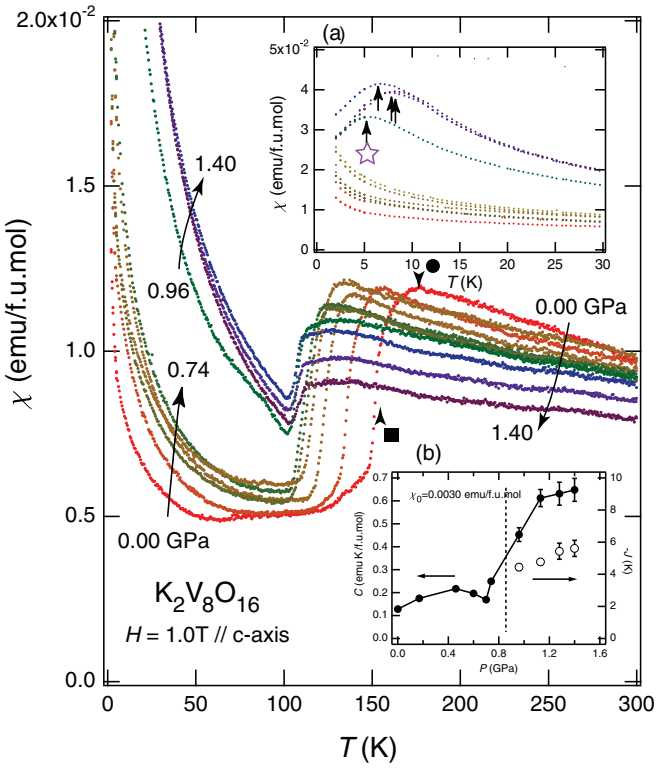

FIG. 4. (Color online) Susceptibility versus temperature (χ-T) curves under several constant pressures up to 1.4 GPa. The rainbow colors show pressure sequences for the measurement of magnetic susceptibility under pressure. The inset (a) shows a macrograph of the low-temperature section (below 30 K) of the χ-T curves. The inset (b) represents the pressure dependencies of the Curie constant C and exchange interaction J estimated from the low-temperature parts of χ-T curves.

measurements of χ make the two-step behavior on χ-T curves clearer; however, the cryogenic condition of MPMS equipped with a high-pressure piston-cylinder cell limits us to the observation of χ-T curves only in the warming process. Thus, the two-step behavior is difficult to observe in this χ-T measurement.

The pressure evolution of χ-T curves (0.00 $\rightarrow$ 1.40 GPa) in the high-temperature metallic phase can be interpreted as a pressure-induced transformation from Curie-Weiss to Pauli paramagnetic metal. In both χ-T and ρ-T measurements, there is no distinct anomaly implying phase transition in the metallic region. Thus, we suppose that there is only one metallic phase within our observed pressure range.

By increasing pressure from 0.0 to 0.74 GPa, a significant drop of the χ-T curve corresponding to the lower step ($T_{\rm CO}^{l}$) of the two-step MIT shifts to a lower temperature as observed in ρ-T measurements. In this pressure region, the Curie tail in the low-temperature χ-T curve is slightly enhanced with increasing pressure. Between 0.74 and 0.96 GPa, a drastic increase of magnetic susceptibility is clearly seen, and the tendency of pressure dependence of MIT, namely pressure evolution of $T_{\rm CO}^{l}$ ($T_{\rm CO}^{h}$ is unclear in this χ measurement), changes at this pressure region. These two aspects, drastic change of magnetic susceptibility and alteration of pressure dependence of MIT, well coincide with those in ρ-T measurements. Therefore, the $P_{\rm c}$ is also observed in this χ-T measurement.

In addition, this χ-T measurement gives us a new aspect which is never seen in ρ-T measurements. The inset (a) shows a macrograph of a low-temperature area (below 30 K) of the χ-T curves. Just above the $P_{\rm c}$, a clear peak on the χ-T curve appears as shown in this inset. From 0.96 up to 1.40 GPa, the peak temperature increases from 5 K to 7 K. Since a recent NMR study[7] has revealed an absence of magnetic order in this high-pressure phase down to 2 K, the origin of these relatively broad peaks would imply short-range antiferromagnetic (sr-AF) ordering well-observed in low-dimensional magnetic systems. Actually, the χ-T curves above the $P_{\rm c}$ can be roughly reproduced by the Bonner-Fisher (BF) expression of $S = 1/2$ uniform spin chain system.[8]

The inset (b) exhibits the pressure dependencies of the Curie constant C (closed circles, left axis) and exchange interaction J (open circles, right axis), corresponding to peak temperatures derived from the BF function analysis. In this analysis, the constant term χ_0 was fixed to 3.0×10^{-3} emu/f.u.mol (namely, 3.75×10^{-4} emu/V·mol) for all the χ-T curves above 0.96 GPa. While the low-temperature χ-T curves for $0 \sim 0.74$ GPa were difficult to fit into simple Curie-Weiss law, $C/(T-\theta)+\chi_0$ (θ: Weiss temperature) in the whole temperature range below $T_{\rm CO}^{l}$, the inverse susceptibility ($1/\chi$-T) curves show good linear behavior in the widest temperature region of $10 \sim 50$ K when the constant term χ_0 is fixed to the same value (3.0×10^{-3} emu/f.u.mol). We have implemented the slope of these $1/\chi$-T curves as C, in spite of the slight enhancement of χ below 10 K and some discrepancy above 50 K.[9]

Below 0.74 GPa, the estimated Curie constants C are less than 0.2 emu·K/f.u.mol. Upon further compression, C shows sudden jump to 0.5 emu·K/f.u.mol at the 0.96 GPa. Above 0.96 GPa, C moderately increases to 0.7 emu·K/f.u.mol at most. This characteristic pressure dependence of C shown in this figure clearly reveals the phase transition at the $P_{\rm c}$ accompanied by an increase in the net magnetic moment of this system. The magnetic properties of this high-pressure phase will be discussed later in relation to the proposed CO models.

IV. DISCUSSION

In order to illustrate several aspects obtained in the ρ-T and χ-T measurements, a P-T phase diagram is drawn as shown in Fig. 5. The two transition temperatures in two-step MIT, namely $T_{\rm CO}^{h}$ and $T_{\rm CO}^{l}$, are shown by circle and square symbols, respectively. These symbols come from only ρ-T measurements because of experimental difficulties on χ-T measurement mentioned above. The open and closed symbols show the transition temperatures observed in cooling and warming processes. The blue and red circle/square symbols are obtained in piston-cylinder/cubic-anvil type pressure experiments, respectively. The open star symbol shows a peak temperature observed in χ-T measurements.

There are three main phases marked by the notations "Metal," "CO1," and "CO2" along with two additional mid-step phases indicated by "CO1′" and "CO2′." As described several times in previous sections, the pressure-induced transition between the CO1 and CO2 phases at the $P_{\rm c}$ is the most

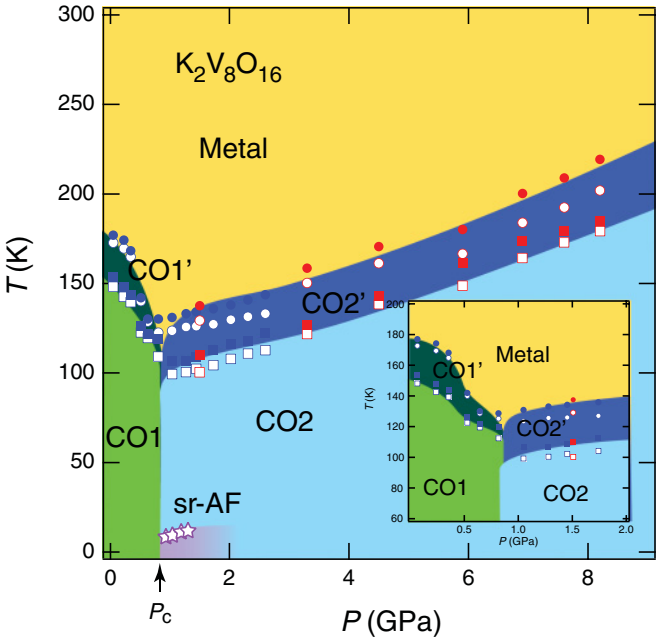

FIG. 5. (Color online) A P-T phase diagram derived from both ρ-T and χ-T measurements. The circle and square symbols represent T_{CO}^{h} and T_{CO}^{l} on ρ-T curves, respectively. Open and closed ones show $T_{\mathrm{CO}}^{h}/T_{\mathrm{CO}}^{l}$ in cooling and warming processes. The blue and red circle/square symbols show results in high-pressure experiments using piston-cylinder and cubic-anvil type pressure cells, respectively. The open star symbol shows a χ-T peak temperature observed in susceptibility measurements.

significant aspect of this work. The phase boundary between these two phases lies at almost constant pressure in a wide temperature range, as shown in Fig. 5, because both ρ-T and χ-T curves dramatically change at the P_{c} across the entire temperature range below T_{CO}^{l}. Just above the P_{c}, a peak in the χ-T curve appears, and the peak temperature slightly increases with increasing pressure. Above 1.4 GPa, it is still difficult to observe the small χ, and consequently the pressure evolution of the peak temperature is still unknown. This is a reason that the boundary of the short-range antiferromagnetic region "sr-AF" is unclear (expressed by gradation) above 1.4 GPa as shown in Fig. 5.

The observed low-dimensional behavior for the high-pressure phase gives us a hint for the CO model. The steep drop of χ at the MIT indicates the formation of spin singlet pairs both in the CO1 and CO2 phases. The first proposed CO model for the ambient low-temperature phase (CO1) contains both dimerized V^{4+} ions and V^{3+} ions, and this model has neither isolated magnetic V^{4+} ions nor V^{3+} ions. Therefore, this CO model could be not true for the CO2 phase because the magnetic moment survives in that phase. Another model proposed from theoretical calculations performed by Ohta *et al.*[10] gives us some valuable information in discussing the high-pressure properties observed in this work. The titled compound has nominally 10 d electrons in a formula unit (f.u.) which includes 8 vanadium atoms (six V^{4+} and two V^{3+}). In the theoretical model, the ferromagnetically coupled V^{4+} ($S = 1/2$) and V^{3+} ($S = 1$) ions mediated via a spin-singlet ($S = 0$) V^{4+}-V^{4+} pair form a 1-dimensional spin chain system as shown in Fig. 8 of Ref. 10. Consequently, two V^{4+} and two V^{3+} ions (spin-singlet unformed) of 8 vanadium ions, namely 6 d electrons, in an f.u. give a net magnetic moment. One can find $C = 2.75$ emu·K/f.u.mol by simple calculation for the Curie constant. Although this model has too large a moment to explain the nonmagnetic aspects of the CO1 phase, it seems to give a hint at the magnetic properties such as large χ and low-dimensional behavior of the χ-T curve in the CO2 phase. The estimated magnetic parameters for the χ-T curve with the largest χ at low temperature are $C = 0.7$ emu·K/f.u.mol and $J \sim -6$ K. Therefore, the pressure-induced magnetic moment in the CO2 phase is still quite small compared to the theoretically expected value. To understand how small it is, we estimated the number of magnetic vanadium ions N in an f.u. The number N is estimated at 2.1/f.u. by assuming that the spin quantum number is $S = 1/2$ (all the magnetic moments come from V^{4+}) and 0.7/f.u. by assuming it is $S = 1$ (from V^{3+}), respectively.

There is one additional model that contains somewhat smaller N. Very recently, Komarek *et al.* determined the crystal structure of the ambient low-temperature phase.[11] Their model, based on structural analysis, contains dimerized V^{4+} and V^{3+} ions and linear chains made of nondimerized V^{4+} ions, which correspond to $N = 4$/f.u, namely $C = 1.5$ emu·K/f.u.mol (four V^{4+} ions of 8 vanadium ions). They also suggested that such a linear chain of nondimerized V^{4+} ions has very large exchange interaction (J). This is much higher than T_{CO}^{h}, and the magnetic susceptibility of the ambient low-temperature (CO1) phase would be the sum of the tail of the BF curve and the contribution of impurities represented as CW law. Such V^{4+} linear chains seem to be responsible for the observed 1-dimensional magnetic behavior of the CO2 phase; however, the observed Curie constant $C = 0.7$ emu·K/f.u.mol is about half the size of the calculated $C = 1.5$ emu·K/f.u.mol. Moreover, the proposed linear V^{4+} chains would have very large J, in contrast to a smaller $J \sim -6$ K for the CO2 phase.

At present, there is no feasible explanation for such small C and J values. The theoretical model, however, is probably acceptable as a basic idea for understanding the spin structure of the CO2 phase, despite the quantitative discrepancy in experimental results. The round χ-T peak and small $J \sim -6$ K can be explained by low dimensionality (probably 1D) of the magnetic system and long-distance spin exchange interaction via singlet spin pair, respectively. Note that the theoretical model assigned ferromagnetic exchange interaction between V^{4+} ($S = 1/2$) and V^{3+} ($S = 1$) ions, which form a 1-dimensional spin system with spin singlet V^{4+} pairs.[10] If this ferromagnetic interaction is turned into an antiferromagnetic one, the two vanadium ions of V^{4+} and V^{3+} may form a low-spin cluster $S_{\mathrm{total}} = 1/2$. This situation results in a relatively small C value, 0.75 emu·K/f.u.mol, closer to the observed $C = 0.7$ emu·K/f.u.mol.

Originally, the theoretical model was proposed for the ambient ground state, CO1 phase in which the $\sqrt{2}a \times \sqrt{2}a \times 2c$ unit cell was observed. At present, there is no information about superperiodicity for the CO2 phase. Therefore, diffraction measurements under pressure are desirable. Additionally, even for the CO1 phase, several kinds of CO structures have been proposed,[1,10,11] and the explicit CO structure is still controversial. Structural information on these ground

states will be beneficial to understanding the physics of this compound.

Correlation between pressure and chemical substitution effects has been frequently discussed. Here, we will compare the pressure effects with the chemical substitution expressed as the chemical formula $K_{2-x}Rb_xV_8O_{16}$. Note that this chemical substitution conserves both the hollandite crystal structure and the nominal valence of vanadium ions. Moreover, with increasing Rb contents x, the lattice expands gradually. Thus, this substitution seems to be interpreted as *negative* pressure. In fact, the metal-insulator transition temperature (probably both T^h_{CO} and T^l_{CO}) increases with expansion of the lattice constants as shown in Fig. 5 of Ref. 12. On the other hand, an unexplainable nature with a *negative* pressure effect is naturally observed in this chemical substitution study. A typical example is an appearance of the tetragonal insulating phase with Rb substitution. This new insulating phase is completely different from the mid-step CO1′ phase because the CO1′ is a monoclinic phase.[3] At present, experimental difficulties on crystal growth of Rb substituted compounds prevent us from observing the detailed relation among the CO1, CO1′, tetragonal insulating, and metallic phases.

The most significant nature of $K_2V_8O_{16}$ is that many kinds of phases appear under pressure and by chemical substitution. This means that there are many kinds of phases in this system which have similar thermodynamic energies. In such a situation, we can expect complexity of phases near P_c as observed in α'-NaV_2O_5[13] and β-$Sr_{0.33}V_2O_5$.[14] This complexity brings us an opportunity to study exotic electric properties near P_c (*non*-ohmic and *non*-activation) such as thyristor behaviors[6] and new physics in the appearance of CO structures.[14]

V. SUMMARY

New pressure-induced phases above 1 GPa were observed in a charge-ordering compound, $K_2V_8O_{16}$. These new phases have relatively strong localized characteristics of carriers and large magnetic moment compared to those in the ambient CO phase. At present, there is no suitable model to explain explicitly these electromagnetic properties under both ambient and high pressure. These observations, however, imply rearrangement of the charge-ordering pattern under pressure. At a minimum, four kinds of CO phases were observed within our experimental capability. Furthermore, a more complex P-T phase diagram will be observed when very precise diffraction experiments are performed under pressure. Such a complex phase diagram given by future work will allow us to view the deep physics concerning charge, orbital, and spin degrees of freedom.

ACKNOWLEDGMENTS

The authors thank Y. Ohta, H. Nakao, Y. Shimizu, and M. Itoh for fruitful discussions. This study is supported by a Grant-in-Aid for Scientific Research (No. 18104008) from the Japan Society for the Promotion of Science.

*yamauchi@issp.u-tokyo.ac.jp

[1] M. Isobe, S. Koishi, N. Kouno, J-I. Yamaura, T. Yamauchi, H. Ueda, H. Gotou, T. Yagi, and Y. Ueda, J. Phys. Soc. Jpn. **75**, 073801 (2006).
[2] W. Abriel, F. Rau, and K. J. Range, Mat. Res. Bull. **14**, 1463 (1979).
[3] M. Isobe, H. Ueda, T. Yamauchi, H. Gotou, T. Yagi, and Y. Ueda (unpublished).
[4] T. Yamauchi and Y. Ueda, Phys. Rev. B **77**, 104529 (2008).
[5] T. Yamauchi, H. Ueda, J. I. Yamaura, and Y. Ueda, Phys. Rev. B **75**, 014437 (2007).
[6] F. Sawano, I. Terasaki, H. Mori, T. Mori, M. Watanabe, N. Ikeda, Y. Nogami, and Y. Noda, Nature (London) **437**, 522 (2005).
[7] Y. Shimizu, K. Okai, M. Itoh, M. Isobe, J-I. Yamaura, T. Yamauchi, and Y. Ueda, Phys. Rev. B , **83**, 155111 (2011).
[8] J. C. Bonner and M. E. Fisher, Phys. Rev. A **135**, 640 (1964); W. E. Estes *et al.*, Inorg. Chem. **17**, 1415 (1978).
[9] Above P_c, there are two ways to obtain the Curie constant C: using the BF function and $1/\chi$-T curves. Naturally, both obtained C values coincide well with each other.
[10] S. Horiuchi, T. Shirakawa, and Y. Ohta, Phys. Rev. B. **77**, 155120 (2008).
[11] A. C. Komarek, Ph.D. thesis, Institute of Physics II, University of Cologne, 2009.
[12] M. Isobe, S. Koishi, S. Yamazaki, J-I. Yamaura, H. Gotou, T. Yagi, and Y. Ueda, J. Phys. Soc. Jpn. **78**, 114713 (2009).
[13] K. Ohwada, Y. Fujii, N. Takesue, M. Isobe, Y. Ueda, H. Nakao, Y. Wakabayashi, Y. Murakami, K. Ito, Y. Amemiya, H. Fujihisa, K. Aoki, T. Shobu, Y. Noda, and N. Ikeda, Phys. Rev. Lett. **87**, 086402-1 (2001).
[14] H. Ueda, T. Yamauchi, K. Ohwada, A. Nakao, Y. Murakami, and Y. Ueda (unpublished).